doi:10.1093/brain/aws036 Brain 2012: 135; 1115–1127 | 1115

BRAIN
A JOURNAL OF NEUROLOGY

Oxidative stress and successful antioxidant treatment in models of RYR1-related myopathy

James J. Dowling,[1,2] Sandrine Arbogast,[3,4] Junguk Hur,[2] Darcee D. Nelson,[5] Anna McEvoy,[1,2] Trent Waugh,[1] Isabelle Marty,[6] Joel Lunardi,[6,7] Susan V. Brooks,[5,8] John Y. Kuwada[9] and Ana Ferreiro[3,4,10,11]

1 Department of Paediatrics, University of Michigan Medical Centre, Ann Arbor, MI 48109-2200, USA
2 Department of Neurology, University of Michigan Medical Centre, Ann Arbor, MI 48109-2200, USA
3 Inserm, U787, Institut de Myologie, Paris, (F-75013), France
4 UPMC, UMR787, Paris, (F-75013), France
5 Department of Biomedical Engineering, University of Michigan Medical Centre, Ann Arbor, MI 48109-2200, USA
6 Grenoble Institut des Neurosciences-INSERM U836, Grenoble, France
7 Biochimie et Génétique Moléculaire, CHU Grenoble/INSERM U836, Grenoble, France
8 Department of Molecular and Integrated Physiology, University of Michigan Medical Centre, Ann Arbor, MI 48109-2200, USA
9 Department Molecular, Cellular, and Developmental Biology, University of Michigan Medical Centre, Ann Arbor, MI 48109-2200, USA
10 AP-HP, Centre de Référence Maladies Neuromusculaires Paris-Est, Groupe Hospitalier Pitié-Salpêtrière, Paris, F-75013, France
11 AP-HP, Service de Pédiatrie, Centre de Référence Maladies Neuromusculaires (GNMH) Hôpital Raymond Poincaré, 92380 Garches, France

Correspondence to: James J. Dowling,
5019 Taubman BSRB, 109 Zina Pitcher Place,
University of Michigan Medical School,
Ann Arbor, MI 48109-2200, USA
E-mail: jamedowl@umich.edu

The skeletal muscle ryanodine receptor is an essential component of the excitation–contraction coupling apparatus. Mutations in *RYR1* are associated with several congenital myopathies (termed RYR1-related myopathies) that are the most common non-dystrophic muscle diseases of childhood. Currently, no treatments exist for these disorders. Although the primary pathogenic abnormality involves defective excitation–contraction coupling, other abnormalities likely play a role in disease pathogenesis. In an effort to discover novel pathogenic mechanisms, we analysed two complementary models of RYR1-related myopathies, the *relatively relaxed* zebrafish and cultured myotubes from patients with RYR1-related myopathies. Expression array analysis in the zebrafish disclosed significant abnormalities in pathways associated with cellular stress. Subsequent studies focused on oxidative stress in *relatively relaxed* zebrafish and RYR1-related myopathy myotubes and demonstrated increased oxidant activity, the presence of oxidative stress markers, excessive production of oxidants by mitochondria and diminished survival under oxidant conditions. Exposure to the antioxidant *N*-acetylcysteine reduced oxidative stress and improved survival in the RYR1-related myopathies human myotubes *ex vivo* and led to significant restoration of aspects of muscle function in the *relatively relaxed* zebrafish, thereby confirming its efficacy *in vivo*. We conclude that oxidative stress is an important pathophysiological mechanism in RYR1-related myopathies and that *N*-acetylcysteine is a successful treatment modality *ex vivo* and in a vertebrate disease model. We propose that *N*-acetylcysteine represents the first potential therapeutic strategy for these debilitating muscle diseases.

Keywords: antioxidant response; myopathies; oxidative stress; neuromuscular disorders

Abbreviations: DCFH = 2′,7′-dichlorofluorescin; DMSO = dimethyl sulphoxide

Received August 12, 2011. Revised November 30, 2011. Accepted December 23, 2011. Advance Access publication March 14, 2012

Introduction

RYR1-related myopathies are a group of disorders associated with causative mutations in the skeletal muscle ryanodine receptor gene *RYR1* (Morrison, 2008). Mutations in *RYR1* have been described in a growing group of skeletal myopathies that include central core disease (Jungbluth, 2007*a*), multiminicore myopathy (Jungbluth, 2007*b*), core-rod myopathy (Hernandez-Lain *et al.,* 2011), centronuclear myopathy (Wilmshurst *et al.,* 2010) and congenital fibre-type disproportion (Clarke *et al.,* 2010). In addition, certain mutations in *RYR1* are associated with malignant hyperthermia susceptibility, a pharmacogenetic condition characterized by muscle rigidity and hyperthermia upon exposure to certain volatile anaesthetics and environmental conditions. Overall, RYR1-related myopathies are the most common congenital myopathy (Amburgey *et al.,* 2011) and are probably the second-most common group of muscle diseases in childhood (Norwood *et al.,* 2009). Most patients with *RYR1* mutations develop clinical signs and symptoms in infancy or early childhood, though RYR1-related myopathies can present in essentially all age groups. Manifestations of disease in childhood include delayed motor milestones, impaired ambulation, extremity muscle weakness, eye movement paralysis, joint contractures, progressive scoliosis, malignant hyperthermia susceptibility and, in some cases, respiratory failure (Zhou *et al.,* 2007). Because of these manifestations, RYR1-related myopathies are associated with significant morbidities and, in some cases, early mortality (Monnier *et al.,* 2009; Hernandez-Lain *et al.,* 2011). To date, no therapies or disease-modifying treatments have proven successful for these severe childhood disorders.

The *RYR1* gene encodes a large, homotetrameric transmembrane ion channel (RyR1) that serves as one of the major intracellular calcium channels in skeletal muscle (Treves *et al.,* 2008). It resides on the terminal sarcoplasmic reticulum in close apposition with the T-tubule. Its primary function is to mediate excitation–contraction coupling, which it does by releasing calcium from the sarcoplasmic reticulum into the cytosol in response to motor neuron-mediated stimulation at the neuromuscular junction (Dulhunty, 2006). RyR1 has additional less well-defined functions, including participation as a dynamic regulator of cellular calcium homeostasis (Zalk *et al.,* 2007).

Both heterozygous (dominant or *de novo*) and recessive mutations have been reported in RYR1-related myopathies. Several mechanisms have been proposed to explain the impact of dominant mutations on RyR1 function (Treves *et al.,* 2008), including chronic calcium leak (Avila and Dirksen, 2001; Zvaritch *et al.,* 2009) and uncoupling of excitation with contraction (Avila *et al.,* 2001; Avila and Dirksen, 2001; Zvaritch *et al.,* 2009). The functional consequences of recessive mutations on RyR1 function are less well understood, though the current prevailing hypothesis is that of a poorly functioning channel on the background of reduced protein levels (Clarke *et al.,* 2010; Wilmshurst *et al.,* 2010). One overall unifying concept is that RYR1-related myopathies are ultimately due to impaired excitation–contraction coupling (Treves *et al.,* 2008), though much is still unclear regarding disease pathogenesis.

RyR1 is involved in several cellular functions in addition to excitation–contraction coupling, and it is thus likely that other abnormalities in addition to excitation–contraction coupling defects contribute to disease pathogenesis. For example, RyR1 is a key mediator of the cellular regulation of calcium homeostasis (Zalk *et al.,* 2007), a process that in turn modulates and influences multiple intracellular signalling pathways and physiological functions. RyR1 is also emerging as an important sensor of cellular redox levels (Pessah *et al.,* 2002). An association between RyR1 dysfunction and redox signalling has recently been demonstrated in two mouse models of malignant hyperthermia (Durham *et al.,* 2008; Giulivi *et al.,* 2011; Wei *et al.,* 2011), a pharmacogenetic condition without muscle weakness that is allelic to RYR1-related myopathies (Rosenberg *et al.,* 2007). In addition, we have recently established the importance of oxidative stress in SEPN1-related myopathy, a congenital myopathy due to defects in selenoprotein-N (SelN) with significant clinical and pathological overlap with RYR1-related myopathies (Arbogast *et al.,* 2009). This overlap, together with the proposed interaction between SelN and RyR1 (Jurynec *et al.,* 2008), suggests that both types of myopathies might share this pathomechanism. To our knowledge, however, redox homeostasis has never been explored either as a disease mechanism or as a therapeutic target in RYR1-related myopathies.

The goal of the present study is to identify novel disease pathways in RYR1-related myopathies as a gateway to therapy development. To this end, we performed RNA expression analysis on a previously characterized zebrafish model of RYR1-related myopathies termed *relatively relaxed* (*ryr*) (Hirata *et al.,* 2007). *Ryr* zebrafish carry a recessive mutation in *ryr1b*, which results in decreased RyR1 levels, impaired excitation–contraction coupling in fast twitch muscles and a severe motor phenotype. Microarray analysis of *ryr* mutants revealed abnormalities in several cellular pathways including oxidative stress, a finding that was validated using several independent experimental measures. To test the relationship of these data to human RYR1-related myopathies, we examined myotubes derived from patient biopsies. Patient myotubes also displayed aberrant oxidative stress, and additionally showed sensitivity to pro-oxidants, findings that were reversed using the antioxidant *N*-acetylcysteine. Treatment of *ryr* zebrafish with *N*-acetylcysteine resulted in restoration of motor function to the level of control fish, thus confirming the potential efficacy of *N*-acetylcysteine as a therapeutic modality *in vivo*. In all, we show that oxidative stress is a relevant pathophysiological mechanism in RYR1-related myopathies and that treatment with *N*-acetylcysteine might represent the first pathophysiology-based therapeutic strategy for these incurable muscle diseases.

Materials and methods

Zebrafish husbandry

Heterozygous *ryr* zebrafish were housed and bred under University Committee on Use and Care of Animals (UCUCA) approved conditions. All zebrafish experiments and procedures were performed according to approved UCUCA specifications.

Zebrafish microarray

RNA was extracted from zebrafish larvae 7 days post-fertilization using an RNeasy® kit (Qiagen; $n = 40$ fish per sample). RNA from each group was amplified, biotin labelled and hybridized to an Affymetrix Zebrafish Genome Array containing 14 900 transcripts (Affymetrix). Intensities of target hybridization to respective probe features were detected by laser scan of the array. Image files were analysed using a local version of the GenePattern genomic analysis platform from the Broad Institute (Reich *et al.*, 2006). Transcripts with a minimum fold expression change of 1.5-fold were selected as differentially expressed genes. Custom Perl scripts were written to obtain the distribution of Gene Ontology terms (http://www.geneontology.org). The Database for Annotation, Visualization and Integrated Discovery (DAVID; http://david.abcc.ncifcrf.gov; Huang da *et al.*, 2009*a*, *b*) was used to identify over-represented Gene Ontology terms and KEGG (Kyoto Encyclopaedia of Genes and Genomes) pathways among the differentially expressed genes ($P < 0.05$).

Quantitative polymerase chain reaction

Quantitative polymerase chain reaction was performed using the SYBR® green supermix (BioRad) and a BioRad iCycler on RNA extracted from zebrafish 7 days post-fertilization. Primers were designed using Primer3 and synthesized by IDT Technologies. Data were normalized to GAPDH levels.

Senescence-associated β-galactosidase assay

The senescence-associated beta galactosidase assay was performed as described by Kishi *et al*. (2008). In brief, zebrafish larvae, 7 days post-fertilization, were fixed overnight in 4% paraformaldehyde and then incubated overnight at 37°C in 5 mM potassium ferrocyanide, 5 mM potassium ferricyanide, 2 mM $MgCl_2$ and 1 mg/ml X-gal in phosphate-buffered saline (pH adjusted to 6.0). Larvae were imaged and photographed under identical conditions using a Nikon AZ100 macroscope. Staining intensity was measured using Adobe Photoshop with a highlighted region over the muscle compartment that was coloured with 25 additive blue colour selection. Obtained pixel values were then analysed using GraphPad Prism.

Zebrafish oxidative stress assays

Zebrafish oxyblot assay

OxyBlot™ analysis to detect protein carbonylation was performed as per the manufacturers protocol (Chemicon) and as previously described (Arbogast *et al.*, 2009). Thirty embryos were collected for each group. Protein (100 μg) was loaded per sample (protein extraction is detailed below). Band density was determined using the BioRad Quantity One® software suite.

Zebrafish 2′,7′-dichlorofluorescin assay to detect intracellular oxidant activity

Fish were euthanized in tricaine and then homogenized in 100 μl buffer (0.32 mM sucrose, 20 mM HEPES, 1 mM MgCl2, 0.5 mM phenylmethanesulphonyl fluoride, pH = 7.4). After centrifugation, supernatants were collected and 20 μl was used per well + 100 μL phosphate-buffered saline and 8.3 μl 2′,7′-dichlorofluorescin (DCFH) diacetate stock (10 mg/ml; Invitrogen). Samples were incubated for 30 min at 37°C and then DCFH fluorescence values were obtained using a Fluoroscan plate reader (485 excitation and 530 emission). Samples were run in triplicate. Values were normalized to protein concentrations.

Zebrafish MitoSOX™ assay

Myofibre cultures were prepared as described previously (Dowling *et al.*, 2009). MitoSOX™ (5 μm; Invitrogen) was applied to freshly isolated fibres for 10 min at 37°C. Cells were washed and then imaged using an Olympus fluorescent microscope. Mean fluorescence intensity of individual myofibres was determined using MetaMorph. Data were quantitated using a one-tailed Student's *t*-test and the GraphPad software program.

Zebrafish western blot analysis

Western blot analysis was performed as previously described (Dowling *et al.*, 2009). Primary antibodies used were: p47-phox (1:250) and actin (1:1000; Santa Cruz Biotech). Secondary antibodies were used at 1:2000 (Santa Cruz Biotech). Blots were developed using Luminglo (Cell Signalling) and a BioRad ChemiDoc™ imager. Band density was determined using the Quantity One® software package (BioRad) and density values analysed using GraphPad Prism.

Zebrafish *N*-acetylcysteine trial

N-acetylcysteine treatment

ryr Embryos were identified by phenotype at 3 days post-fertilization. Embryos (both *ryr* and unaffected clutchmates) were then incubated in either dimethyl sulphoxide (DMSO) alone (0.1%) or DMSO + *N*-acetylcysteine (200 μm). Solutions were changed daily. The effect of *N*-acetylcysteine on cellular stress was measured using the senescence associated β-galactosidase assay, and the effect of oxidative stress was measured using the DCFH assay.

Behavioural monitoring

Zebrafish behavioural parameters were defined using the Noldus activity monitoring system. For this, fish 7 days post-fertilization were placed in six-well dishes and then put into the monitoring system with the light box on. Fish behaviour was recorded with an infrared light source for 5 min. Each fish was measured with three trials (separated by 5 min) and the behavioural parameters recorded reflect an average of these three trials.

Contractile properties

At 6 days post-fertilization, *ryr* and unaffected clutchmates (previously incubated in either 0.1% DMSO or DMSO + *N*-acetylcysteine) were tested over a 2-day period. Larvae were mounted into an experimental chamber with one end attached to a stationary post and the other end to a force transducer (400A, Aurora Scientific). Muscle contraction was accomplished by electrical stimulation. The following parameters were assayed: peak force normalized to cross-sectional muscle area, time to peak force, half relaxation time and fatigue and recovery. See Supplementary material for detailed methods.

Electron microscopy

At 7 days post-fertilization, zebrafish were fixed overnight at 4°C in Karnovsky's fixative and then processed for electron microscopy. Samples were visualized on a Philips CM-100 transmission electron microscope. Microscopy was performed at the University of Michigan Microscopy and Imaging Laboratory.

Human RYR1-related myopathy myotube methodology

Human myotubes

Myocytes were obtained from diagnostic muscle biopsies after informed consent in agreement with local ethics committees, following previously described procedures (Arbogast *et al.,* 2009). For all experiments, cells from four controls, five patients with core myopathy (RYR1-related myopathies) and three patients with malignant hyperthermia sensitivity were used. Details of the specific mutations in *RYR1* for each patient are listed in Supplementary Table 1.

Oxyblot assay on human myotubes

The oxyblot assay was performed and interpreted as previously described (Arbogast *et al.,* 2009). In brief, 15 μg protein was loaded per sample. Muscle protein samples without the derivatization step were used as negative controls. After scanning with an imaging densitometer, optical densities of protein bands were quantified using ImageJ software. Total protein carbonylation optical density in a given sample was calculated by adding optical densities of individual carbonylated protein bands.

2′,7′-dichlorofluorescin assay on human myotubes

The DCFH assay was performed as previously described (Arbogast *et al.,* 2009). Human myotubes were incubated with DCFH-diacetate (50 μM) for 30 min allowing probe equilibration, and oxidized DCF was measured from representative areas using an epifluorescence microscope (Olympus). Mean fluorescence intensity was obtained from 10 images containing at least 10 myotubes and used as an individual value to calculate the global mean and standard error values.

Chemical inhibitor treatments

The DCFH assay was used to evaluate the effects of the NADPH oxidase inhibitor apocynin (100 μM) or the cyclo-oxygenase inhibitor indomethacin (100 μM; Sigma-Aldrich). Cells treated with DMSO were used as a control.

Real-time polymerase chain reaction analysis of messenger RNA levels in human myotubes

Total RNA from human myotubes was prepared using an RNeasy® kit (Qiagen) and reverse transcribed using the SuperScript III Kit (Invitrogen). Gene expression was then determined using the RT^2 Human Oxidative Stress Profiler™ PCR Expression Array (SABiosciences Inc.) according to the manufacturer's instructions.

Western blot analysis of RYR1-related myopathy myotubes

Western blot analysis on protein extracts from human myotubes was performed as previously described (Arbogast *et al.,* 2009). The following primary antibodies were used: gp91 phox and p67 phox (Santa Cruz) and tubulin (Sigma-Aldrich). Band intensity was measured and compared, with values normalized to tubulin levels.

MitoSOX assay on human myotubes

MitoSOX™ red was administered as described by the manufacturer (Invitrogen). Myotubes were loaded with MitoSOX™ (5 μM) for 45 min at 37°C. Mean fluorescence intensity for each well was obtained from five images containing at least 10 myotubes and used as an individual value to calculate the global mean and standard error values.

Myotube survival assay

Approximately 90% confluent cells were treated for 24 h with 100 μM H_2O_2 (Sigma-Aldrich) in culture medium. The number of viable and non-viable cells was counted using a light microscope, taking exclusion of trypan blue as an index of cell viability. Furthermore, the total number of cells per well was verified after fixation by staining with propidium iodide (Sigma-Aldrich).

N-acetylcysteine treatment of human myotubes

The effect of *N*-acetylcysteine treatment was assessed using oxyblot analysis, DCFH assay and examination of cell survival. For oxyblot and DCFH assays, cells were treated for 24 h with *N*-acetylcysteine (5 mM) and then the assays performed as above. Cell survival was measured on myotubes treated with *N*-acetylcysteine for 20 min before treatment with 100 μM H_2O_2.

Data analysis

Analysed data are represented as mean ± S.E.M. Where stated, statistical significance was determined by using Student's *t*-test and the SigmaStat program (Jandel).

Results

Pathways associated with cellular stress are altered in *ryr* zebrafish

The *ryr* zebrafish (Hirata *et al.,* 2007) has an insertion mutation in the *ryr1b* gene, the sole zebrafish RyR1 expressed in fast muscle. In the homozygous state, this mutation results in significant loss of RyR1 expression (residual expression = 1–10% of normal), impaired RyR1 function and a stereotypically abnormal swimming behaviour (easily identified by 3 days post-fertilization). To determine novel pathogenic pathways associated with loss of RyR1 function, we performed comparative microarray expression analysis on RNA isolated from *ryr* zebrafish at 7 days post-fertilization and age-matched wild-type siblings. Six hundred and twenty transcripts were identified in *ryr* zebrafish in which expression levels increased by at least 50% over that of wild-type siblings. Of these, 532 were associated with 512 Entrez gene IDs while 82 were unannotated (Supplementary Fig. 1). Molecular function pathway analysis revealed changes in a broad range of cellular functions (Supplementary Fig. 2), and we noted that several of the significantly mis-expressed pathways were associated with redox and cellular homeostasis and the cellular response to stress (Fig. 1A). To validate our microarray findings, we examined expression of two genes (*saa1* and *moxd1*) associated with cellular stress that were differentially expressed in mutant versus wild-type zebrafish. Quantitative reverse transcriptase-polymerase chain reaction confirmed a 1.9-fold increase in *saa1* expression and a 1.6-fold increase in *moxd1* (Fig. 1B). To validate that cellular stress was increased *in vivo*, we measured senescence-associated β-galactosidase activity at pH = 6.0, an assay previously shown to be a measure of cellular stress in zebrafish (Kishi *et al.,* 2008). We observed a significant increase in β-galactosidase activity in *ryr* zebrafish (Fig. 1C and D), confirming abnormal cellular stress in this model of RYR1-related myopathies.

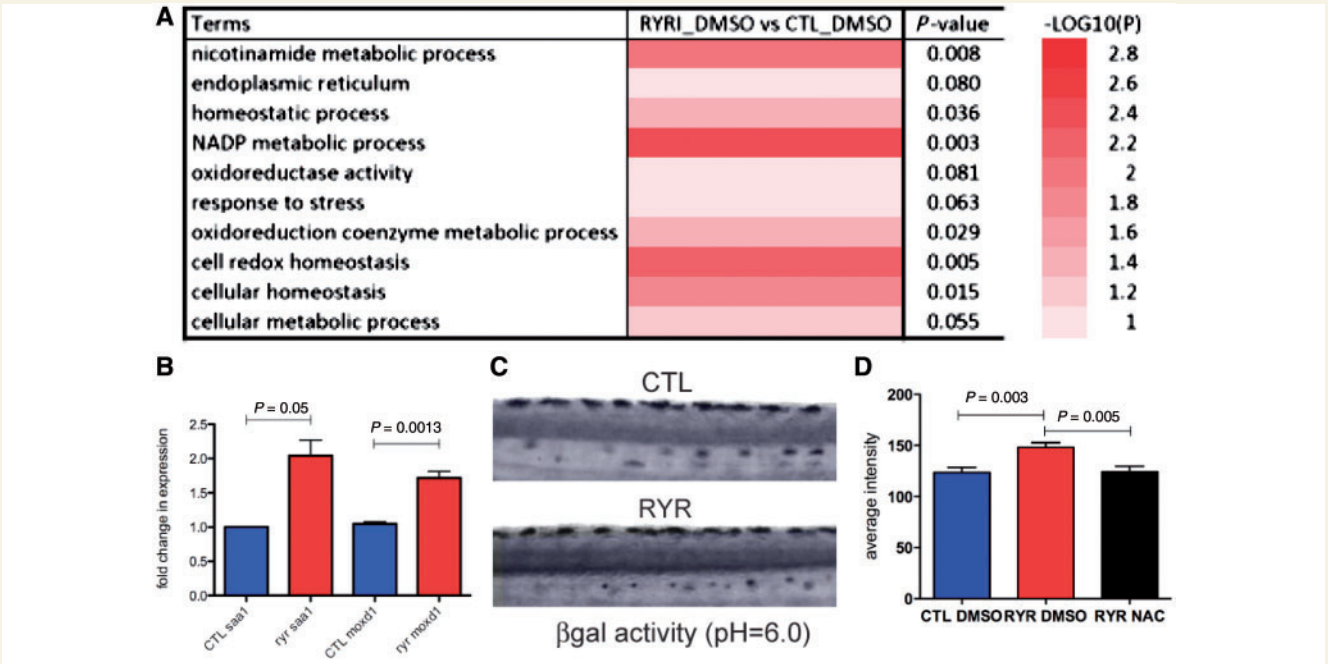

Figure 1 Pathways associated with cellular and oxidative stress are misregulated in *ryr* zebrafish. (**A**) Comparative microarray expression analysis of RNA from *ryr* zebrafish versus control age-matched clutchmates. Significant changes of 1.5-fold or greater in several pathways associated with cellular and oxidative stress were detected. Complete array results are presented in Supplementary Fig. 1. (**B**) Quantitative polymerase chain reaction validation of microarray data for two genes (*saa1* and *moxd1*) associated with cellular stress. Three independent samples from each condition were tested for each gene. (**C** and **D**) Senescence associated beta galactosidase (βgal) activity (measured at pH = 6.0), a marker for cellular stress, as measured at 7 days post-fertilization in control (CTL) and *ryr* (RYR) larvae. Representative images are shown in (**C**). Quantitation of βgal activity (mean optical density) revealed significant increased levels in *ryr*s (**D**): CTL DMSO = 123.4 ± 5.1 and RYR DMSO = 148.0 ± 4.7 ($n = 8$, $P = 0.003$). *N*-acetylcysteine (NAC) treatment restored activity to control levels. RYR *N*-acetylcysteine = 124.1 ± 5.5. ($n = 8$, $P = 0.005$ compared with RYR DMSO).

ryr Zebrafish show increased oxidant activity and markers of oxidative stress

Given the previously reported involvement of RyR1 in redox homeostasis, we focused specifically on oxidative stress as a cause of overall cellular stress. Oxidative stress was assayed in whole zebrafish using two different approaches. First, we used oxyblot analysis to measure the level of carbonylated (oxidated) proteins. Carbonylation, a post-translational modification, correlates with oxidative stress due to reactive oxygen species and represents a well-established oxidative stress marker (Arbogast *et al.*, 2009). We found a significant increase in protein carbonylation in whole *ryr* zebrafish protein extracts from larvae at 7 days post-fertilization when compared with wild-type siblings (Fig. 2A and B).

We next used the *in situ* DCFH assay, a validated measure of overall intracellular oxidant activity (Chen *et al.*, 2010). DCF fluorescence emission in *ryr* zebrafish was significantly increased to 2.1-fold the levels measured in control clutchmates (Fig. 2C). To determine the relative specificity of this observation to alteration of RyR1 function, we performed the DCFH assay on two other zebrafish models of muscle disease, the '*sapje*' model of dystrophin mutation (Bassett *et al.*, 2003) and the '*candyfloss*' model of merosin deficiency (Hall *et al.*, 2007). '*Sapje*' zebrafish had normal DCF emission levels, whereas '*candyfloss*' zebrafish displayed a modest (1.5-fold) increase compared with control clutchmates. Importantly, DCF emission levels in *ryr* were significantly increased in comparison to either of the two models, suggesting that increased basal oxidant activity and oxidative stress may be uniquely abnormal in the setting of RyR1 dysfunction (Fig. 2C).

Basal oxidant activity and oxidative stress markers are increased in myotubes from patients with RYR1-related myopathies

To confirm that oxidative stress is involved in RYR1-related myopathies, and that this mechanism is not exclusively associated with RyR1 quantitative abnormalities as observed in the *ryr* zebrafish, we analysed differentiated cultured muscle cells from human patients expressing dominant or recessive missense *RYR1* mutations. Our cohort contained five independent sets of myotubes derived from diagnostic muscle biopsies from four dominant/*de novo* patients and one recessive patient. These samples were analysed comparatively with myotubes obtained from four age-paired healthy individuals and from three patients with malignant hyperthermia susceptibility but no myopathy (Supplementary Table 1). We examined overall intracellular

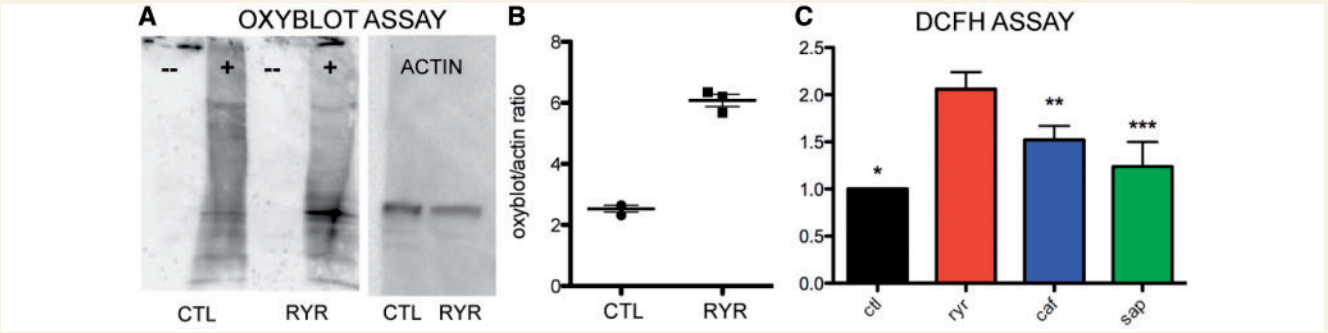

Figure 2 Oxidative stress and increased oxidative markers in *ryr* zebrafish. Oxyblot analysis of total protein extracts from 7 days post-fertilization control (CTL) and *ryr* (RYR) zebrafish. (**A**) Representative blot from single pools of fish ($n = 40$). Oxyblot (± 2,4-dinitrophenylhydrazine reagent) is *left*, western blot using actin antibody *right*. (**B**) Quantitation of oxyblot data expressed as a ratio of oxyblot band average intensity to actin band intensity. Data are from three independent experiments. CTL = 2.5 ± 0.1 versus RYR = 5.7 ± 0.2, $P = 0.0001$. (**C**) DCFH assay as performed on pools of 7 days post-fertilization zebrafish (40 fish per pool) from the following strains: control clutchmates (ctl), *ryr*, *candyfloss* (*caf*) and *sapje* (*sap*). Data are expressed as fold-change from control values. *ryr* = 2.1, *caf* = 1.5 and *sap* = 1.2. *P*-values = 0.0005 (**ryr* versus ctl), 0.03 (***ryr* versus *caf*), 0.02 (****ryr* versus *sap*), 0.006 (*caf* versus ctl) and 0.17 (*sap* versus ctl).

oxidant activity and oxidative stress markers using oxyblot analysis and the DCFH assay (Fig. 3). As with *ryr* zebrafish, oxyblot analysis on protein extracts from patient myotubes revealed a significant increase in carbonylated protein content compared to controls in all samples examined (Fig. 3A and B). With the DCFH assay, RYR1-related myopathy myotubes showed under basal conditions a significant increase of intracellular oxidant activity compared to control myotubes (Fig. 3C). Of note, while the mean oxidant activity was robustly and significantly increased in patient cells, individual results in this set of samples showed a high dispersion compared to control samples, suggesting that different mutations may be associated with different degrees of increase in oxidant activity. Taken together, the oxyblot analysis and the DCFH assay revealed that both basal oxidant activity and markers of oxidative stress are significantly increased in myotubes from patients with RYR1-related myopathies. Interestingly, we also observed increases in oxidant levels and oxidative stress in myotubes derived from patients with *RYR1* mutations and malignant hyperthermia susceptibility but no obvious clinical myopathy (Supplementary Fig. 3). This is consistent with previous redox-related data from malignant hyperthermia susceptibility mouse models (Durham *et al.*, 2008; Giulivi *et al.*, 2011; Wei *et al.*, 2011), thus supporting the validity of our *ex vivo* model.

Oxidative stress in RYR1-related myopathies is not due to major defects in antioxidant defence gene expression

Oxidative stress results from a loss of balance between production of reactive oxygen species and buffering, which can be either due to the overproduction of reactive oxygen species or due to a defect in antioxidant defence mechanisms. To better understand the mechanism(s) underlying oxidative stress in RYR1-related myopathies, we examined the expression of several genes associated with oxidative stress and antioxidant defence. We first directly measured the levels of selenoprotein-N (SEPN1) messenger RNA, because SelN has been implicated in the interplay between RyR1 and redox homeostasis (Jurynec *et al.*, 2008; Arbogast and Ferreiro, 2010). We found no difference in the expression of SEPN1 or in the levels of the other antioxidant selenoproteins SEPP1 and SELS4 (Table 1). We next quantified the expression of other genes implicated in antioxidant defence using an oxidative stress profiler array. We observed no changes in the expression of antioxidant defence genes; in particular, no changes were noted for catalase, superoxide dismutase 1, mitochondrial superoxide dismutase and extracellular superoxide dismutase (Table 1). We also examined expression of these genes in malignant hyperthermia susceptibility patient myotubes and in the *ryr* zebrafish and found no statistical change in their levels when compared with control groups (Table 1 and data not shown). These results suggest that the oxidative stress observed in our models of RYR1-related myopathies is due to excessive production of oxidants as opposed to decreased antioxidant capacity.

Oxidative stress in RYR1-related myopathies is related to mitochondrially derived reactive oxygen species

We next explored sources of excessive production of reactive oxygen species in RYR1-related myopathies. One potential source, because of its localization in the sarcoplasmic reticulum near RyR1, is the NADPH oxidase complex (Hidalgo *et al.*, 2006). We did not, however, see significant changes in messenger RNA levels of any of its subunits (Table 1). As transcriptional regulation is not the only means of NADPH oxidase regulation, we also measured protein levels of NADPH oxidase subunits and found gp91-phox to be increased in myotubes of patients with RYR1-related myopathies compared to controls and p47-phox to be increased in *ryr* zebrafish (Supplementary Fig. 4). To examine the functional relevance of this increase, we inhibited the activity

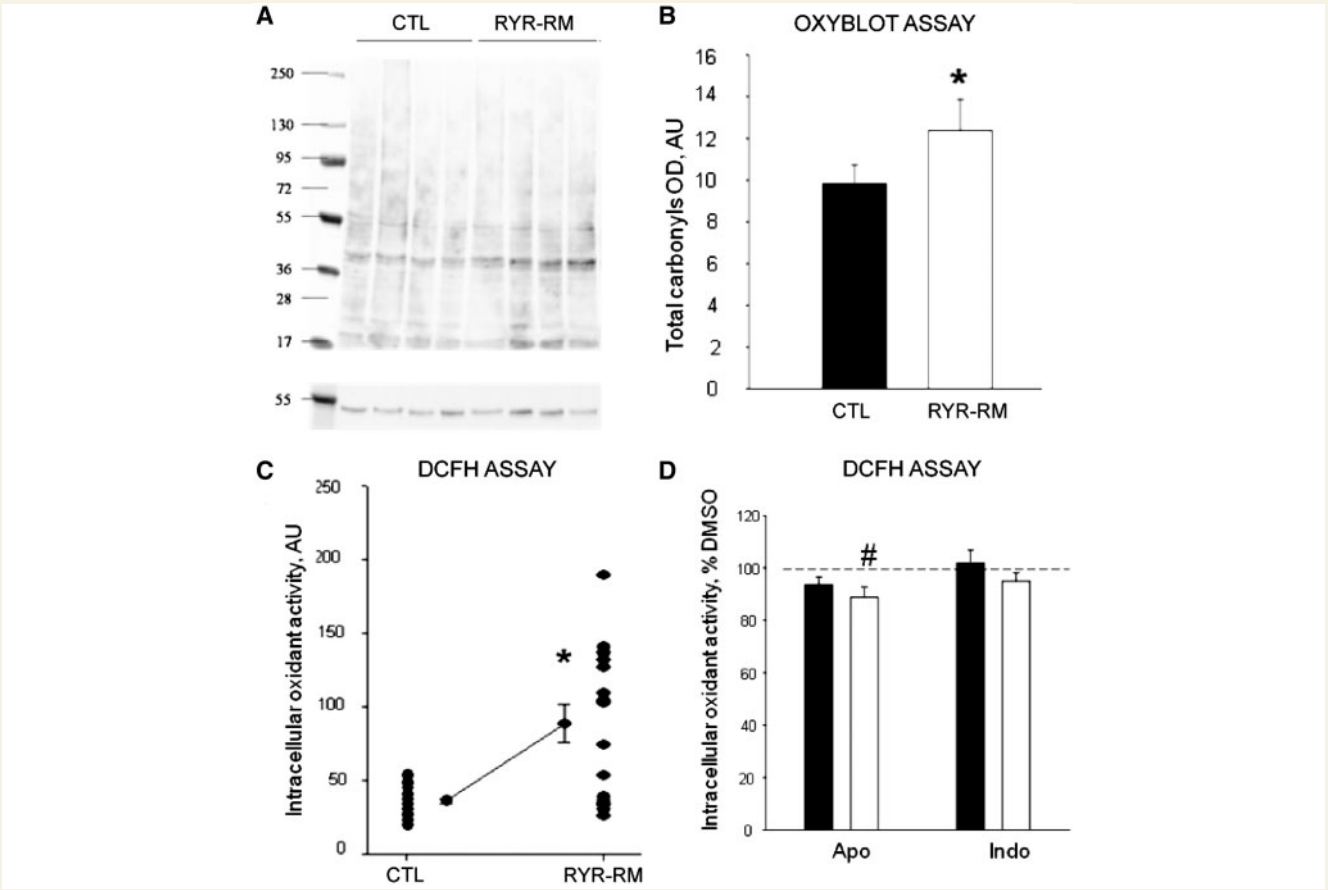

Figure 3 Oxidative stress and increased oxidative markers in RYR1-related myopathy (RYR1-RM) myotubes. (**A**, **B**) Increased oxidative stress markers as measured using oxyblot assay. (**A**) Representative oxyblot from control (CTL) and RYR1-related myopathy myotubes. (**B**) Quantitation of mean total carbonyls showing a significant increase in RYR1-related myopathy myotubes as compared to control (*$P < 0.001$). (**C**) Basal oxidant activity expressed in arbitrary units (AU) was measured by use of the DCFH assay in myotubes from RYR1-related myopathy ($n = 8$) and control subjects ($n = 4$). A significant increase of $69 \pm 20\%$ was observed in patient myotubes (asterisks). Each dot represents the average value of the fluorescence intensity of 10 myotubes. (**D**) Quantitation of oxidant activity using DCFH assay from control (black) and RYR-RM (white) myotubes after incubation with apocynin (Apo, $n = 19$) or indomethacin (indo, $n = 19$). Results are reported as per cent of oxidant activity compared with DMSO treated myotubes. A small but significant decrease was observed in RYR1-related myopathy myotubes after apocynin treatment ($^{\#}P < 0.001$).

Table 1 Expression changes for oxidative stress and antioxidant related genes in human myotubes

Gene Name	Protein	Description	CM		MHS	
			Fold-Regulation	*P*	Fold-Regulation	*P*
SEPN1	SelN	Selenoprotein N	1.03	0.930	−1.09	0.476
SELS	SelS	Selenoprotein S	1.48	0.158	−2.72	0.079
SEPP1	SelP	Selenoprotein P, plasma, 1	1.27	0.623	−2.15	0.153
CAT	Catalase	Catalase	−1.01	0.978	−3.32	0.102
SOD1	Cu/Zn SOD	Superoxide dismutase 1, soluble	1.15	0.398	−1.77	0.429
SOD2	MnSOD	Superoxide dismutase 2, mitochondrial	−1.64	0.250	2.92	0.369
SOD3	EC-SOD	Superoxide dismutase 3, extracellular	−2.50	0.284	−3.28	0.215
CYBA	p22	Cytochrome b-245, alpha polypeptide	1.50	0.484	−3.19	0.220
NCF1	P47	Neutrophil cytosolic factor 1	−1.02	0.982	−1.51	0.817
NCF2	P67-PHOX	Neutrophil cytosolic factor 2	1.26	0.647	1.46	0.680
CYBB	GP91 PHOX	NADPH oxidase 2 cytochrome b(558) subunit beta	1.07	0.192	**1.66**	**0.014**
PTGS2	COX2	Prostaglandin-endoperoxide synthase 2	**544.37**	**0.001**	**95.51**	**0.011**
MOXD1	MOXD1	Monooxygenase, DBH-like 1	**3.45**	**0.005**	**4.19**	**0.001**

Fold-regulation represents biologically meaningful fold-change results. Fold-change values > 1 indicate positive regulation or an upregulation, and the fold-regulation is equal to the fold-change. Fold-change values < 1 indicates a negative or downregulation, and the fold-regulation is the negative inverse of the fold-change. All values were normalized to those from control myotubes. CM = myotubes of patients with RYR1-related myopathy; MHS = malignant hyperthermia susceptibility. Bold indicates $P < 0.05$.

of NADPH oxidase and then measured the change in overall oxidant levels using the DCFH assay. Inhibition of NADPH oxidase with apocynin resulted in a modest ($-13 \pm 4\%$) reduction in the overall amount of reactive oxidant species in the patient myotubes; however, levels were still significantly elevated when compared with controls treated with apocynin (Fig. 3D). We thus concluded that NADPH oxidase contributes only modestly to the overall oxidant activity in RYR1-related myopathy myotubes, and that additional sources of reactive oxygen species must exist in these cells.

Another potential source of oxidative stress is the prostaglandin-dependent cyclo-oxygenase PTGS2. We examined this pathway because the *PTGS2* gene was significantly upregulated in patient myotubes (500-fold increase, $P = 0.0001$; Table 1). To study the potential functional impact of this pathway, we applied the prostaglandin inhibitor indomethacin to the myotubes. Indomethacin, however, did not alter the intracellular oxidant activity in patient myotubes when compared with controls (Fig. 3D), indicating that the PTGS2 cyclo-oxygenase likely does not contribute to overall oxidant activity in the myotubes and is thus not the main source of reactive oxygen species in RYR1-related myopathies.

Given that mitochondria are one of the main subcellular producers of calcium-dependent reactive oxygen species, we lastly examined mitochondrially derived reactive oxygen species as an oxidant source. To do this, we use the MitoSOX^{TM} reagent, a live cell redox sensor that specifically identifies mitochondrial-generated superoxide. MitoSOX^{TM} fluorescence was significantly increased in RYR1-related myopathy myotubes when compared with controls ($+24 \pm 5\%$ of controls; Fig. 4A). We examined MitoSOX^{TM} staining in isolated zebrafish myofibres as well and found that staining intensity in *ryr* myofibres was 1.5 times greater than that observed in controls (Fig. 4B and C). To then evaluate the relationship of mitochondrially derived reactive oxygen species to the overall burden of oxidative stress in RYR1-related myopathies, we exposed human myotubes to *N*-acetylcysteine, a potent antioxidant known to act primarily in the mitochondrial reactive oxygen species pathway. Incubation with *N*-acetylcysteine had a significant effect on overall oxidative stress, reducing basal intracellular oxidant activity by 51% (Fig. 5A) and restoring carbonylated protein levels in RYR1-related myopathy myotubes to values even lower than those of controls (Fig. 5B and C).

Treatment of *ryr* larvae with *N*-acetylcysteine similarly resulted in a resolution of cellular stress. This was demonstrated by restoration of senescence-associated β-galactosidase activity to baseline levels (Fig. 1D) as well as resolution of a subset of altered gene expression changes (including *moxd1* and *saa1*) as revealed by microarray analysis (Supplementary Fig. 6) and quantitative polymerase chain reaction (Supplementary Fig. 7A). Oxidative stress in *ryr* zebrafish, as determined using the DCFH assay, was restored to control levels (Supplementary Fig. 7B). Taken together, our data from the human *ex vivo* model and from the *ryr* zebrafish point to the mitochondria as the significant source of oxidative stress in RYR1-related myopathies and reveal the ability of *N*-acetylcysteine to reduce overall cellular and oxidative stress.

RYR1-related myopathy myotubes are sensitive to oxidants and protected by treatment with *N*-acetylcysteine

To determine the functional consequences of oxidative stress on RYR1-related myopathy muscle cells, we challenged them with the oxidant H_2O_2. Exposure of control cells to H_2O_2 resulted in a mild decrease in cell survival (Fig. 5D). Conversely, exposure of patient myotubes to the same oxidant conditions caused a significant and dramatic decrease in survival both in RYR1-related myopathies (Fig. 5D) and in malignant hyperthermia susceptibility (Supplementary Fig. 5). We next examined the impact of antioxidant treatment on this sensitivity to oxidant exposure. We chose to use *N*-acetylcysteine because of its ability (described above) to restore oxidant levels to those of control cells. We found that pretreatment of myotubes with *N*-acetylcysteine significantly and

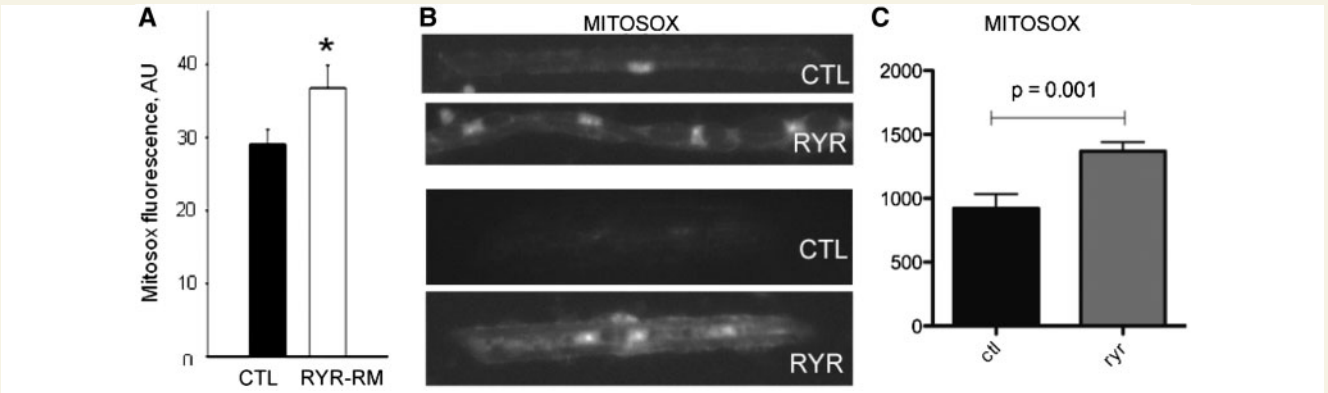

Figure 4 Increased mitochondrial ROS production in RYR1-related myopathy (RYR1-RM) myotubes and *ryr* zebrafish. Mitochondrial reactive oxygen species was measured using the MitoSOX^{TM} reagent. (**A**) Mitochondrial reactive oxygen species production as determined by MitoSOX^{TM} fluorescence under basal conditions in control and RYR1-related myopathy myotubes. RYR1-related myopathy myotubes showed a significant increase in mitochondrial reactive oxygen species production (measured in arbitrary units, AU) ($26\% \pm 6.7\%$ increase, $P < 0.05$). (**B**) Representative images from myofibres isolated from control (CTL) and *ryr* (RYR) zebrafish stained with MitoSOX. (**C**) Quantitation of intensity of MitoSOX staining in zebrafish myofibres. Values (in arbitrary units) were 920.6 ± 114.4 (CTL) and 1369.0 ± 73.1 (RYR), with $n = 11$ fibres measured per condition and $P = 0.001$.

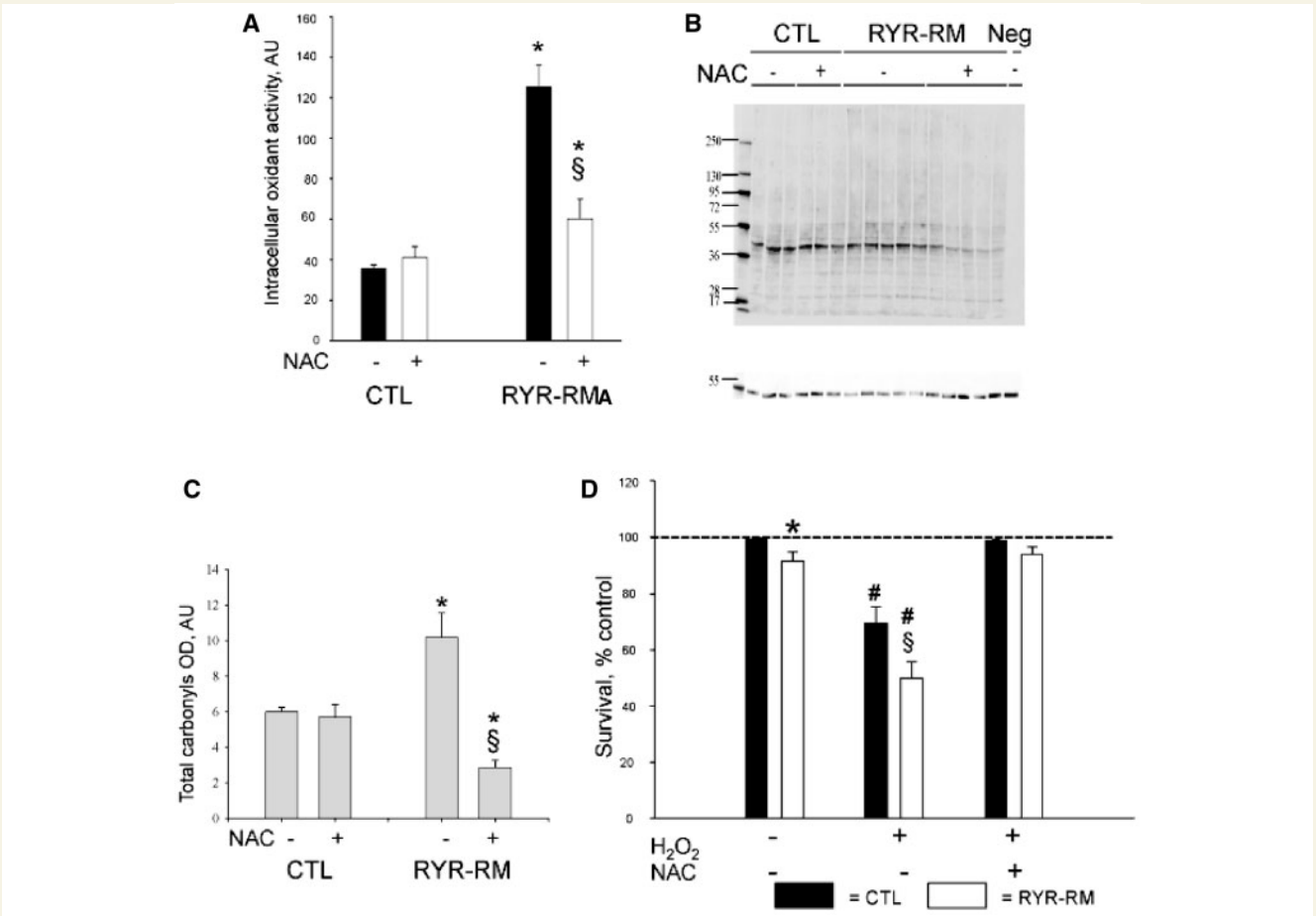

Figure 5 *N*-acetylcysteine (NAC) reduces oxidative stress and improves survival in RYR1-related myopathy (RYR1-RM) myotubes. (**A**) Intracellular oxidant activity in control and RYR1-related myopathy myotubes with or without exposure to 5 mM *N*-acetylcysteine. *N*-acetylcysteine significantly reduced Intracellular oxidant activity in RYR1-related myopathy myotubes. (**B** and **C**) Oxyblot analysis of control (CTL) and RYR1-related myopathy myotubes with or without exposure to 5 mM *N*-acetylcysteine. *N*-acetylcysteine significantly reduced total carbonyl content in RYR1-related myopathy myotubes, restoring it to the levels of control. Representative blot depicted in (B). Quantitation in (C; measured in mean total carbonyl optical density) ($^{*}P = 0.05$ in untreated cells for RYR1-related myopathy versus CTL and for RYR1-related myopathy *N*-acetylcysteine treated versus untreated) ($^{\S}P < 0.05$ versus CTL). (**D**) Myotubes were exposed to H_2O_2 with or without *N*-acetylcysteine pretreatment. RYR1-related myopathy myotubes displayed significantly decreased survival (-48% versus -31%, $^{\#}P < 0.05$). Pretreatment with *N*-acetylcysteine prevented oxidant-induced cell death in both CTL and RYR1-related myopathy myotubes.

completely protected RYR1-related myopathy and malignant hyperthermia susceptibility myotubes from cell death induced by H_2O_2 ($P < 0.05$; Fig. 5D and Supplementary Fig. 5).

Treatment with *N*-acetylcysteine restores motor function and improves muscle histopathology in *ryr* zebrafish

The effectiveness of *N*-acetylcysteine in preventing oxidant-induced cell death in RYR1-related myopathy myotubes led us to hypothesize that *N*-acetylcysteine may improve the overall clinical phenotype *in vivo* in RYR1-related myopathies. We tested this hypothesis by analysing the effect of *N*-acetylcysteine on motor behaviour in *ryr* zebrafish. The basic treatment strategy was as follows: (i) we identified *ryr* larvae at 3 days post-fertilization based on their easily recognizable motor phenotype; (ii) we then separated fish into four treatment categories: unaffected sibs without treatment (CTL + 0.1% DMSO), siblings treated with *N*-acetylcysteine (CTL + *N*-acetylcysteine), *ryr* without treatment (RYR + 0.1% DMSO) and *ryr* with *N*-acetylcysteine (RYR + *N*-acetylcysteine); (iii) treatment was initiated at 3 days post-fertilization; and (iv) end-points were measured after 4 days of therapy (7 days post-fertilization). Conditions (including water temperature and pH) were otherwise identical between treatment groups. The *N*-acetylcysteine concentration used (200 μM, diluted in 0.1% DMSO) was based on previous studies of *N*-acetylcysteine in cell culture and our own establishment of the maximal tolerated dose in control fish, which was determined based on the absence of morphological abnormalities and on 100% survival for the treatment time course (data not shown).

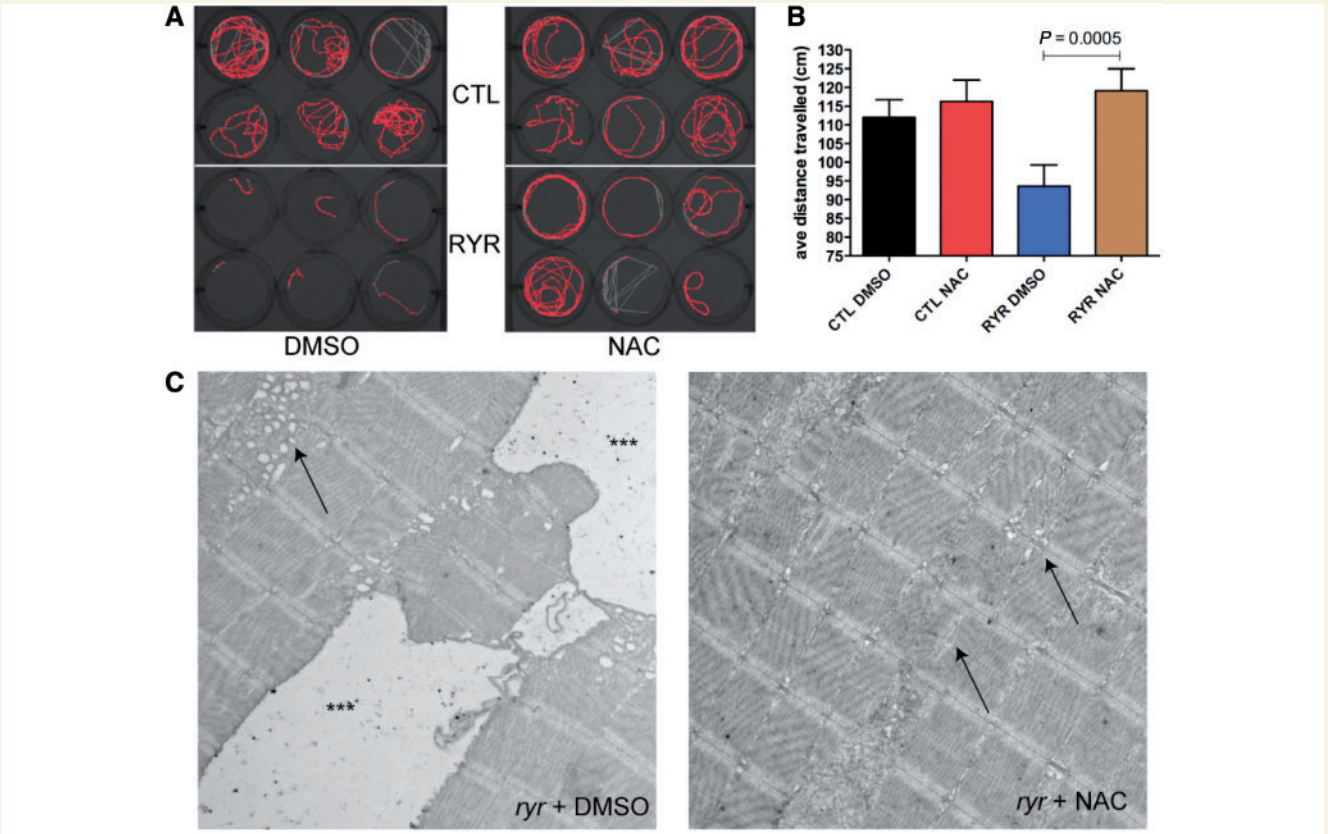

Figure 6 *N*-acetylcysteine treatment ameliorates aspects of the ryr motor phenotype. (**A**) Representative screen capture from 5 min of monitoring using the Noldus activity monitoring system. Each well represents a single fish, with the red signal corresponding to a map of fish movement during the 5-min epoch. The depicted experiment is from fish treated for 4 days in either 0.1% DMSO (*left* panel) or 200 μm *N*-acetylcysteine (*right* panel). The top six wells in each are control clutchmates (CTL), while bottom six wells are *ryr* zebrafish (RYR). (**B**) Quantitation of the average distance travelled during 5 min of monitoring (recorded in triplicate) for 7 days post-fertilization larvae treated for 4 days with DMSO or *N*-acetylcysteine. (**C**) Electron microscopic analysis on 7 days post-fertilization *ryr* larvae incubated for 4 days in either 0.1% DMSO or DMSO + *N*-acetylcysteine ($n = 5$ per group). (*Left*) Prominent pathologic changes were observed in *ryr* skeletal muscle, including large areas of what are likely swollen longitudinal sarcoplasmic reticulum (triple asterisks) as well as smaller areas of dilated membranes that represent abnormal terminal sarcoplasmic reticulum (arrow). (*Right*) Pathological changes were significantly reduced in *ryr* zebrafish exposed to *N*-acetylcysteine. The large dilated membrane compartments were not found, and the presence of swollen terminal sarcoplasmic reticulum was reduced (right arrow). The muscle was not entirely normal, as small areas of sarcomeric disruption were still observed (left arrow). Scale bar = 1 μm.

We measured two primary motor/behavioural end-points: swim velocity and distance travelled. These measurements were obtained using the Noldus activity monitoring system, which uses an infrared camera to track fish movement over defined trial periods. Swim velocity is determined in cm/s and only calculated for the portions of the time interval when the fish are moving, whereas distance travelled reflects the total number of centimetres travelled during the trial. We examined these parameters at 7 days post-fertilization (a time when control fish move relatively constantly), with the velocity and distance travelled per fish reflecting the average of three consecutive 5-min trials. As expected, untreated *ryr* zebrafish moved significantly less than control clutchmates (in cm; Fig. 6A; CTL + DMSO versus RYR + DMSO, 112.0 ± 4.7 versus 93.6 ± 5.7; $P = 0.073$; $n = 73$). On the other hand, *N*-acetylcysteine treatment resulted in a large and robust effect on the distance travelled by *ryr* zebrafish, restoring their movements to the levels of *N*-acetylcysteine exposed control fish (Fig. 6A; CTL + *N*-acetylcysteine versus RYR + *N*-acetylcysteine, 116.2 ± 5.7 versus 119.1 ± 5.9; $P = 0.73$; $n = 73$). Swim velocity also significantly differed between control and *ryr* zebrafish; however, unlike the total distance travelled, no change in velocity was detected between treated and untreated *ryr* zebrafish. The values obtained for each larva were (in cm/s): CTL + DMSO = 1.29 ± 0.31; CTL + *N*-acetylcysteine = 1.32 ± 0.31; RYR + DMSO = 1.03 ± 0.10 and RYR = 1.09 ± 0.17. Taken together, these results suggest that *N*-acetylcysteine improves the motor phenotype by increasing the endurance of *ryr* zebrafish.

In an attempt to understand why *N*-acetylcysteine improves motor function in *ryr* zebrafish, we analysed the contractile properties of the skeletal muscle in whole mount zebrafish preparations ($n = 9$ for all measurements). The following parameters, measured at 6–8 days post-fertilization, were evaluated and compared between DMSO- and *N*-acetylcysteine-treated larvae: peak force

generation (Supplementary Fig. 8A), time to reach peak force (Supplementary Fig. 8B), rate of relaxation after twitch contraction (Supplementary Fig. 8C) and fatigue and recovery of force generation (Supplementary Fig. 8D). As expected, significant differences in all parameters were observed between control and *ryr* larvae incubated in 0.1% DMSO. However, no differences were detected between DMSO- and *N*-acetylcysteine-treated *ryr* zebrafish. *N*-acetylcysteine treatment thus does not alter several basic aspects of the contractile properties of *ryr* muscle; data were consistent with the ability of *N*-acetylcysteine to improve distance travelled but not swim velocity.

Histopathological alterations have previously been reported in the skeletal muscle of *ryr* zebrafish. To evaluate the effect of *N*-acetylcysteine treatment on these abnormalities, we examined *ryr* larvae after 4 days of treatment using electron microscopy. In untreated *ryr* zebrafish at Day 7 of life, we observed several distinct histological defects, the most dramatic of which were large areas of swollen and dilated organelles compatible with sarcoplasmic reticulum (Fig. 6C). These areas were found along the length of the myofibre and were of two qualities. The first (marked with triple asterisks) were very large areas with a paucity of electron dense material; the second (marked with an arrow) were pockets of swollen sarcoplasmic reticulum in the vicinity of the junction with T-tubules (i.e. triads). These findings were observed in all untreated *ryr* zebrafish examined ($n = 5$). Other changes included abnormal appearance of some myonuclei and small areas of disrupted myofibrils (likely small 'minicores'; data not shown). In contrast to the untreated mutants, *ryr* zebrafish treated with *N*-acetylcysteine had a dramatic reduction of the pathological areas of dilated and swollen sarcoplasmic reticulum. Four of five larvae examined displayed no evidence of these aberrant structures (Fig. 6D). Instead, skeletal muscle from *ryr* zebrafish treated with *N*-acetylcysteine had essentially normal-appearing sarcoplasmic reticulum and triads (arrowheads). Muscle from *N*-acetylcysteine treated *ryr* zebrafish was not completely normal, as rare areas of myofibril disorganization were observed (arrow). Of note, no evidence of myofibre death, as assessed using acridine orange staining, was observed in either DMSO or *N*-acetylcysteine-treated *ryr* zebrafish ($n = 20$; data not shown).

Discussion

RYR1-related myopathies are a common group of childhood muscle disorders associated with severe morbidity and early mortality that currently have no treatment. Although RYR1-related myopathies are primarily due to abnormal excitation–contraction coupling and altered calcium homeostasis, the impact of secondary/downstream mechanisms on disease is largely unexplored. Using a zebrafish model of recessive RYR1-related myopathies (Hirata *et al.,* 2007) and a complementary *ex vivo* model of human myotubes from patients with *RYR1* mutations, we provide the first evidence implicating oxidative stress as an important pathophysiological mechanism in RYR1-related myopathies. We further reveal that *N*-acetylcysteine is a successful treatment *ex vivo* and in an *in vivo* model system and propose that this antioxidant represents the first viable potentially pathophysiology-based treatment for these devastating disorders.

Translational impact: antioxidant therapy for RYR1-related myopathies

The main import of our study concerns its translational application, through the identification and validation *ex vivo* and *in vivo* of a first pathophysiology-based pharmacological treatment for RYR1-related myopathies using the antioxidant *N*-acetylcysteine. We demonstrate a robust and significant effect of antioxidant treatment on the motor phenotype in the *relatively relaxed* zebrafish. Specifically, untreated fish show a significant deficit in time spent moving/swimming, while treated fish move as frequently as wild-type fish, observations that suggest that the effect of antioxidant therapy is to improve endurance. In healthy humans, increased oxidative stress is associated with increased muscle fatigue and decreased endurance (Powers and Jackson, 2008), and *N*-acetylcysteine has been shown to delay or improve these changes (McKenna *et al.,* 2006). It therefore is logical that *ryr* zebrafish, because of their increased basal levels of oxidative stress, have impaired endurance that is significantly improved when they are exposed to *N*-acetylcysteine.

In an attempt to better understand the relationship between *N*-acetylcysteine treatment and phenotypic improvement, we tested several avenues where *N*-acetylcysteine may have potential impact. The majority of these measures did not reveal a significant change between untreated and treated *ryr* zebrafish. In particular, assessment of skeletal muscle contractile properties did not show a difference with *N*-acetylcysteine. This was not entirely surprising as *in vitro* studies of myofibres have shown that, at least in some contexts, fatigue-related force reduction is not improved by *N*-acetylcysteine exposure (Bruton *et al.,* 2008). One area where *N*-acetylcysteine did show improvement was with muscle histopathology. Untreated *ryr* muscle has abundant areas of dilated and swollen organelles, which are significantly reduced in number in treated fish. The exact reason for and significance of this improvement deserves further investigation.

One of the most important findings from our study is the demonstration for the first time of increased oxidative stress in myotubes from patients with RYR1-related myopathies. The data from our zebrafish studies provide compelling preclinical evidence for the presence of abnormal oxidative stress and for the potential impact of antioxidant therapy. However, without a clinical correlation, it would be difficult to know the true relevance of these findings to human muscle disease. The fact that we observed abnormalities in oxidative stress in a diverse group of samples, i.e. patients with myopathy and a range of different RYR1 mutations (as well as patients with malignant hyperthermia susceptibility and no weakness), implies that regardless of mechanism, aberrant oxidative stress is a consistent phenomenon in this group of diseases. Of note, fatigue and decreased exercise tolerance are common complaints in patients with RYR1-related myopathies (personal observations). It is tempting to speculate that these symptoms are due to the increased oxidative stress we observed in patient myotubes, and that *N*-acetylcysteine

therapy may alleviate these symptoms in patients with RYR1 mutations. *N*-acetylcysteine is one of the rare antioxidant drugs approved for human use, has been clinically shown to inhibit muscle fatigue in healthy adults (Reid *et al.,* 1994) and has no serious side effects when administered at the established dosage (Mant *et al.,* 1984; Reid *et al.,* 1994). In addition, chronic *N*-acetylcysteine therapy has been used in combination with metronidazole to ameliorate symptoms in both a mammalian model and in five paediatric patients with ethylmalonic encephalopathy, a severe metabolic disease with mitochondrial dysfunction (Viscomi *et al.,* 2010). These observations, together with its *ex vivo* and *in vivo* efficiency on our models of RYR1-related myopathies, pave the way to a first therapeutic approach to this severe and relatively prevalent group of inherited muscle disorders and open interesting perspectives for the other skeletal muscle and heart conditions in which RyR1 dysfunction is primarily or secondarily involved. *N*-acetylcysteine is already being considered for therapeutic efficacy in SEPN1-related myopathy, which, as mentioned, shares significant clinical overlap with RYR1-related myopathies and probably has aspects of secondary RyR1 dysfunction.

Mechanisms of oxidative stress in RYR1-related myopathies

An important unresolved question that emerges from our experimentation is how *RYR1* mutations associated with myopathy lead to oxidative stress. We have identified the mitochondria as the likely source of reactive oxygen species production in our models. This observation makes intuitive sense given (i) the close proximity of the mitochondria and the terminal sarcoplasmic reticulum (where RyR1 resides); and (ii) the fact that the mitochondria are the main source of reactive oxygen species production in the setting of altered calcium homeostasis. It remains to be determined at a mechanistic level how diminished RyR1 function, especially when associated with decreased RyR1 expression and/or diminished calcium release, leads to mitochondrially derived reactive oxygen species generation. One possible explanation in this context is that excessive accumulation of calcium in the sarcoplasmic reticulum (due to impaired release through RyR1) causes increased calcium flux into the adjacent mitochondria (via the IP3 receptor or through the newly identified mitochondrial calcium uniporter; Baughman *et al.,* 2011), and then this increased mitochondrial calcium leads to the production of reactive oxygen species. Future experimentation will be necessary to test potential mechanisms.

Although our study introduces the first association between RYR1-related myopathies and oxidative stress, a link between RyR1 dysfunction and oxidative stress has been previously described in the setting of malignant hyperthermia susceptibility without muscle weakness due to *RYR1* mutation. *RYR1* mutations causing malignant hyperthermia susceptibility alone result in hyperexcitable channels. As determined from a series of elegant studies using two murine models, oxidative stress in malignant hyperthermia susceptibility is due to a feed-forward loop of episodic excessive calcium release from hyperexcitable RyR1 channels causing increased reactive oxygen species/reactive nitrogen species production and leading to further activation of RyR1 and additional pathological calcium release. Given, however, that RYR1-related myopathies are associated with impaired channel function as opposed to channel hyperexcitability, it is likely that the changes that lead to oxidative stress in these diseases are distinct from those observed with malignant hyperthermia susceptibility alone. Interestingly, mitochondrially derived reactive oxygen species are also a key component of oxidative stress in malignant hyperthermia susceptibility models; thus, despite likely involving different initiating events (hyperexcitability instead of diminished function), the ultimate source of pathologically accumulated reactive oxygen species appears to be the same in both diseases. Of note, the alterations in oxidative stress levels were not significantly different between myotubes from patients with RYR1-related myopathies and those from patients with malignant hyperthermia susceptibility only.

Conclusion

We provide evidence from a vertebrate model of RYR1-related myopathies that basal oxidative stress is increased and that treatment with the antioxidant *N*-acetylcysteine can reduce cellular and oxidative stress and improve muscle histology and overall motor phenotype. We validate the relevance of these findings by showing that oxidative stress is increased in patient myotubes from a variety of RYR1-related myopathies, and that *N*-acetylcysteine fully restores their cellular phenotype. Based on our findings, we conclude that oxidative stress is an important disease pathomechanism in RYR1-related myopathies, and that antioxidant therapy is a promising avenue for treatment intervention for these severe childhood muscle diseases.

Acknowledgements

The authors thank Angela Busta, Andrew Vreede and Philicia Duncan for technical assistance and Jack Iwashyna for statistical assistance. We thank Caroline Serreri, Charline Ramahefasolo and the DNA and Cell Bank (Genethon, Evry, France) for technical assistance with cell culture and Drs Norma Romero and Bridgette Estournet for assistance with patient diagnoses.

Funding

National Institutes of Health (1K08AR054835 to J.J.D., R01NS54731 to J.Y.K. and AG-020591 to S.V.B.); the Child Neurology Foundation (J.J.D.) and the National Science Foundation (NSF 0725976 to J.Y.K.). Additional support was from Endostem (FP7 grant to S.A.), the ANR (Agence Nationale pour la Recherche, MyCa grant), the INSERM (Institut National de la Santé et la Recherche Médicale) and the AP-HP (Assistance Publique-Hôpitaux de Paris, Contrat d'Interface to A.F.).

Supplementary material

Supplementary material is available at *Brain* online.

References

Amburgey K, McNamara N, Bennett LR, McCormick ME, Acsadi G, Dowling JJ. Prevalence of congenital myopathies in a representative pediatric united states population. Ann Neurol 2011; 70: 662–5.

Arbogast S, Beuvin M, Fraysse B, Zhou H, Muntoni F, Ferreiro A. Oxidative stress in SEPN1-related myopathy: from pathophysiology to treatment. Ann Neurol 2009; 65: 677–86.

Arbogast S, Ferreiro A. Selenoproteins and protection against oxidative stress: selenoprotein N as a novel player at the crossroads of redox signaling and calcium homeostasis. Antioxid Redox Signal 2010; 12: 893–904.

Avila G, Dirksen RT. Functional effects of central core disease mutations in the cytoplasmic region of the skeletal muscle ryanodine receptor. J Gen Physiol 2001; 118: 277–90.

Avila G, O'Brien JJ, Dirksen RT. Excitation–contraction uncoupling by a human central core disease mutation in the ryanodine receptor. Proc Natl Acad Sci USA 2001; 98: 4215–20.

Bassett DI, Bryson-Richardson RJ, Daggett DF, Gautier P, Keenan DG, Currie PD. Dystrophin is required for the formation of stable muscle attachments in the zebrafish embryo. Development 2003; 130 (23): 5851–60.

Baughman JM, Perocchi F, Girgis HS, Plovanich M, Belcher-Timme CA, Sancak Y, et al. Integrative genomics identifies MCU as an essential component of the mitochondrial calcium uniporter. Nature 2011; 476: 341–5.

Bruton JD, Place N, Yamada T, Silva JP, Andrade FH, Dahlstedt AJ, et al. Reactive oxygen species and fatigue-induced prolonged low-frequency force depression in skeletal muscle fibres of rats, mice and SOD2 overexpressing mice. J Physiol 2008; 586: 175–84.

Chen X, Zhong Z, Xu Z, Chen L, Wang Y. 2′,7′-Dichlorodihydrofluorescein as a fluorescent probe for reactive oxygen species measurement: forty years of application and controversy. Free Radic Res 2010; 44: 587–604.

Clarke NF, Waddell LB, Cooper ST, Perry M, Smith RL, Kornberg AJ, et al. Recessive mutations in RYR1 are a common cause of congenital fiber type disproportion. Hum Mutat 2010; 31: E1544–50.

Dowling JJ, Vreede AP, Low SE, Gibbs EM, Kuwada JY, Bonnemann CG, et al. Loss of myotubularin function results in T-tubule disorganization in zebrafish and human myotubular myopathy. PLoS Genet 2009; 5: e1000372.

Dulhunty AF. Excitation-contraction coupling from the 1950s into the new millennium. Clin Exp Pharmacol Physiol 2006; 33: 763–72.

Durham WJ, Aracena-Parks P, Long C, Rossi AE, Goonasekera SA, Boncompagni S, et al. RyR1 S-nitrosylation underlies environmental heat stroke and sudden death in Y522S RyR1 knockin mice. Cell 2008; 133: 53–65.

Giulivi C, Ross-Inta C, Omanska-Klusek A, Napoli E, Sakaguchi D, Barrientos G, et al. Basal bioenergetic abnormalities in skeletal muscle from ryanodine receptor malignant hyperthermia-susceptible R163C knock-in mice. J Biol Chem 2011; 286: 99–113.

Hall TE, Bryson-Richardson RJ, Berger S, Jacoby AS, Cole NJ, Hollway GE, et al. The zebrafish candyfloss mutant implicates extracellular matrix adhesion failure in laminin alpha2-deficient congenital muscular dystrophy. Proc Natl Acad Sci USA 2007; 104: 7092–7.

Hernandez-Lain A, Husson I, Monnier N, Farnoux C, Brochier G, Lacene E, et al. De novo RYR1 heterozygous mutation (I4898T) causing lethal core-rod myopathy in twins. Eur J Med Genet 2011; 54: 29–33.

Hidalgo C, Sanchez G, Barrientos G, Aracena-Parks P. A transverse tubule NADPH oxidase activity stimulates calcium release from isolated triads via ryanodine receptor type 1 S -glutathionylation. J Biol Chem 2006; 281: 26473–82.

Hirata H, Watanabe T, Hatakeyama J, Sprague SM, Saint-Amant L, Nagashima A, et al. Zebrafish relatively relaxed mutants have a ryanodine receptor defect, show slow swimming and provide a model of multi-minicore disease. Development 2007; 134: 2771–81.

Huang da W, Sherman BT, Lempicki RA. Bioinformatics enrichment tools: paths toward the comprehensive functional analysis of large gene lists. Nucleic Acids Res 2009a; 37: 1–13.

Huang da W, Sherman BT, Lempicki RA. Systematic and integrative analysis of large gene lists using DAVID bioinformatics resources. Nat Protoc 2009b; 4: 44–57.

Jungbluth H. Central core disease. Orphanet J Rare Dis 2007a; 2: 25.

Jungbluth H. Multi-minicore disease. Orphanet J Rare Dis 2007b; 2: 31.

Jurynec MJ, Xia R, Mackrill JJ, Gunther D, Crawford T, Flanigan KM, et al. Selenoprotein N is required for ryanodine receptor calcium release channel activity in human and zebrafish muscle. Proc Natl Acad Sci USA 2008; 105: 12485–90.

Kishi S, Bayliss PE, Uchiyama J, Koshimizu E, Qi J, Nanjappa P, et al. The identification of zebrafish mutants showing alterations in senescence-associated biomarkers. PLoS Genet 2008; 4: e1000152.

Mant TG, Tempowski JH, Volans GN, Talbot JC. Adverse reactions to acetylcysteine and effects of overdose. Br Med J (Clin Res Ed) 1984; 289: 217–9.

McKenna MJ, Medved I, Goodman CA, Brown MJ, Bjorksten AR, Murphy KT, et al. *N*-acetylcysteine attenuates the decline in muscle Na+,K+-pump activity and delays fatigue during prolonged exercise in humans. J Physiol 2006; 576 (Pt 1): 279–88.

Monnier N, Laquerriere A, Marret S, Goldenberg A, Marty I, Nivoche Y, et al. First genomic rearrangement of the RYR1 gene associated with an atypical presentation of lethal neonatal hypotonia. Neuromuscul Disord 2009; 19: 680–4.

Morrison L. Unraveling RYR1 mutations and muscle biopsies. Neurology 2008; 70: 99–100.

Norwood FL, Harling C, Chinnery PF, Eagle M, Bushby K, Straub V. Prevalence of genetic muscle disease in Northern England: in-depth analysis of a muscle clinic population. Brain 2009; 132 (Pt 11): 3175–86.

Pessah IN, Kim KH, Feng W. Redox sensing properties of the ryanodine receptor complex. Front Biosci 2002; 7: a72–9.

Powers SK, Jackson MJ. Exercise-induced oxidative stress: cellular mechanisms and impact on muscle force production. Physiol Rev 2008; 88: 1243–76.

Reich M, Liefeld T, Gould J, Lerner J, Tamayo P, Mesirov JP. GenePattern 2.0. Nat Genet 2006; 38: 500–1.

Reid MB, Stokic DS, Koch SM, Khawli FA, Leis AA. *N*-acetylcysteine inhibits muscle fatigue in humans. J Clin Invest 1994; 94: 2468–74.

Rosenberg H, Davis M, James D, Pollock N, Stowell K. Malignant hyperthermia. Orphanet J Rare Dis 2007; 2: 21.

Treves S, Jungbluth H, Muntoni F, Zorzato F. Congenital muscle disorders with cores: the ryanodine receptor calcium channel paradigm. Curr Opin Pharmacol 2008; 8: 319–26.

Viscomi C, Burlina AB, Dweikat I, Savoiardo M, Lamperti C, Hildebrandt T, et al. Combined treatment with oral metronidazole and *N*-acetylcysteine is effective in ethylmalonic encephalopathy. Nat Med 2010; 16: 869–71.

Wei L, Salahura G, Boncompagni S, Kasischke KA, Protasi F, Sheu SS, et al. Mitochondrial superoxide flashes: metabolic biomarkers of skeletal muscle activity and disease. FASEB J 2011.

Wilmshurst JM, Lillis S, Zhou H, Pillay K, Henderson H, Kress W, et al. RYR1 mutations are a common cause of congenital myopathies with central nuclei. Ann Neurol 2010; 68: 717–26.

Zalk R, Lehnart SE, Marks AR. Modulation of the ryanodine receptor and intracellular calcium. Annu Rev Biochem 2007; 76: 367–85.

Zhou H, Jungbluth H, Sewry CA, Feng L, Bertini E, Bushby K, et al. Molecular mechanisms and phenotypic variation in RYR1-related congenital myopathies. Brain 2007; 130 (Pt 8): 2024–36.

Zvaritch E, Kraeva N, Bombardier E, McCloy RA, Depreux F, Holmyard D, et al. Ca2+ dysregulation in Ryr1(I4895T/wt) mice causes congenital myopathy with progressive formation of minicores, cores, and nemaline rods. Proc Natl Acad Sci USA 2009; 106: 21813–8.